

Citation for published version:

Ning, J, Wang, W, Ge, G, Chu, P, Long, F, Yang, Y, Peng, Y, Feng, L, Ma, X & James, TD 2019, 'Target Enzyme-Activated Two-Photon Fluorescent Probes: A Case Study of CYP3A4 Using a Two-Dimensional Design Strategy', *Angewandte Chemie - International Edition*, vol. 58, no. 29, pp. 9959-9963.
<https://doi.org/10.1002/anie.201903683>

DOI:

[10.1002/anie.201903683](https://doi.org/10.1002/anie.201903683)

Publication date:

2019

Document Version

Peer reviewed version

[Link to publication](#)

This is the peer reviewed version of the following article: J. Ning, W. Wang, G. Ge, P. Chu, F. Long, Y. Yang, Y. Peng, L. Feng, X. Ma, T. D. James, *Angew. Chem. Int. Ed.* 2019, 58, 9959, which has been published in final form at <https://doi.org/10.1002/anie.201903683>. This article may be used for non-commercial purposes in accordance with Wiley Terms and Conditions for Self-Archiving.

University of Bath

Alternative formats

If you require this document in an alternative format, please contact:
openaccess@bath.ac.uk

General rights

Copyright and moral rights for the publications made accessible in the public portal are retained by the authors and/or other copyright owners and it is a condition of accessing publications that users recognise and abide by the legal requirements associated with these rights.

Take down policy

If you believe that this document breaches copyright please contact us providing details, and we will remove access to the work immediately and investigate your claim.

Targeted Enzyme Activated Two-Photon Fluorescent Probes: A Case Study of CYP3A4 Using a Two-Dimensional Design Strategy

Jing Ning, Wei Wang, Guangbo Ge, Peng Chu, Lei Feng,* Feida Long, Yongliang Yang,* Yulin Peng, Xiaochi Ma*, and Tony D. James

Abstract: Nowadays, the rapid development of fluorescent probe for monitoring target enzyme is still a great challenge, due to the lack of efficient way to optimize a specific fluorophore. Herein, a practical two-dimension molecular strategy was designed to construct an isoform-specific probe for CYP3A4, a key cytochrome P450 isoform responsible for oxidize most of clinical drugs. In first dimension of the molecular design, using ensemble-based virtual screening, the potential two-photon fluorophore substrate (**NN**) for CYP3A4 was effectively filtered. For second dimension by chemical modification, various substituent groups were introduced to candidate **NN** for optimizing the isoform-selectivity and reactivity. Finally, with ideal selectivity and sensitivity, **NEN** was successfully applied to real-time detect CYP3A4 in living cells and zebrafish, thereby providing an efficient tool for quantitative tracking of CYP3A4 activity in complex biological systems. These findings suggested that our strategy is practical to develop an isoform-specific probe for a target enzyme.

Cytochrome P450 monooxygenase (CYP) is a superfamily of oxidative enzymes that metabolizes thousands of endogenous and exogenous substances through alkyl carbon and aromatic ring hydroxylation, O- and N-dealkylation, and epoxidation.^[1] CYP3A4 is

regarded as the most important CYP isoform in human, due to its high abundance in liver as well as broad substrate spectrum which contributes to that metabolism of more than 50% of clinical drugs.^[2,3] Unfortunately, CYP3A4 activity can be modulated by many clinical drugs, thereby frequently causing unfavorable drug-drug interactions (DDI), further leading to altered clinical outcomes or even life-threatening adverse reactions.^[4] Additionally, a significant inter-individual variability of CYP3A4 activity is frequently reported, arising from a number of sources including genetic polymorphism and the response to environmental influences.^[5] These factors have greatly limited the understanding of the precise role of CYP3A4 in drug metabolism and DDI, as a result, negatively impacted clinical medication safety and effectiveness.

To accurately characterize CYP3A4 activity, sensitive technologies capable of real-time monitoring CYP3A4 activity are urgently needed. Traditional detection methods mainly rely upon mass spectrometry or high-performance liquid chromatography,^[6,7] while they are not compatible with living cell or *in vivo* applications. Two-photon (TP) fluorescence microscopy, by virtue of its higher sensitivity, real-time spatial high-resolution imaging, and amenability to deep-tissue bioimaging, has shed new light on monitoring target enzyme activity in complex systems.^[8,9] However, there is still no TP fluorescent probe developed for real-time and selective imaging of endogenous CYP3A4 activity in living systems.

Previous attempts to develop a fluorescent probe for CYP3A4 were based on a dealkylation mechanism to release a detectable moiety. The O-alkyl derivatives of coumarin, resorufin, and fluorescein were designed and synthesized, but met with limited success in isoform selectivity.^[10] The leading cause for the poor specificity of these probes is that dealkylation usually is a preferential reaction for CYP1A1 and CYP1A2 rather than CYP3A4, especially with polycyclic aromatic compounds.^[11] In the light of the extraordinary ability of CYP3A4 to mediate the aromatic hydroxylation,^[12] we hypothesized that the high specific probe of CYP3A4 might be obtained by tuning the fluorescence-generation using site specific hydroxylation to 'Switch-ON' the fluorophore.

Nowadays, the greatest challenge in designing an isoform-selective and sensitive activity-based fluorescent probe is how to effectively find a specific fluorophore and optimize the structure.^[13] A simple 'lock and key' method to acquire a rational fluorophore is urgently needed. Herein, we developed a two-dimensional design strategy to achieve an overall "best-fit" molecular tool for selective detection of CYP3A4, which would provide the molecular design strategy from scratch virtual screening of putative two-photon fluorescent substrates (Scheme 1 and Figure S1).^[14] For the first design dimension, an in-house docking program FIPSDock was used to perform the constrained ensemble-based hydroxylation of the specific sites on fluorophore. For sensitive fluorescence detection, the introduction of a hydroxyl to fluorophore substrates producing significant fluorescence response, was set as the restrictive reaction and thus was limited to the catalytic site. To ensemble the conformational changes of CYP3A4 upon binding with the different sizes of substrates, we obtained twelve crystallographic human CYP3A4 structures from the Protein Data screening against the Bank (PDB code: 1TQN, 1W0F, 1W0G, 2J0D, 2V0M, 3TJS,

[*] Dr. J. Ning,^[†] P. Chu,^[†] Dr. L. Feng, Y. L. Peng, Prof. X. C. Ma
College of Integrative Medicine, The National & Local Joint
Engineering Research Center for Drug Development of
Neurodegenerative Disease, College of Pharmacy
Dalian Medical University
Dalian 116044, China
E-mail: leifeng@mail.dlut.edu.cn (L. Feng); maxc1978@163.com (X. C. Ma)

P. Chu,^[†] Dr. L. Feng, F. D. Long, Prof. Y. L. Yang
Center for Molecular Medicine, School of Life Science and
Biotechnology, State Key Laboratory of Fine Chemicals
Dalian University of Technology
Dalian 116024, China
E-mail: everbright99@foxmail.com (Y. L. Yang)

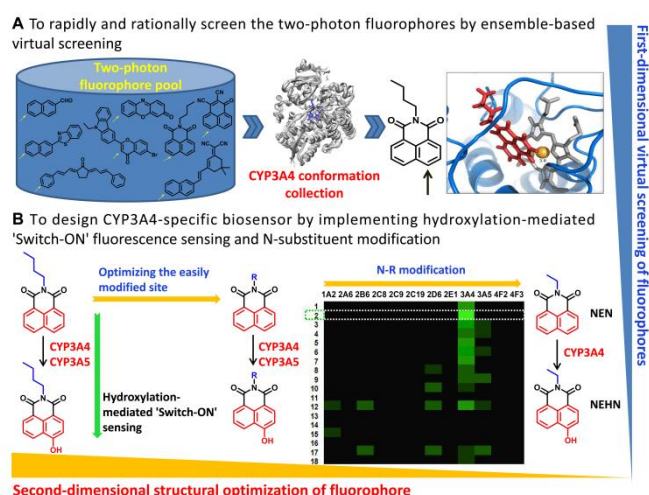
Prof. X. C. Ma
Jiangsu Key Laboratory of New Drug Research and Clinical
Pharmacy
Xuzhou Medical University
Xuzhou 221004, China.
E-mail: maxc1978@163.com (X. C. Ma)

Prof. W. Wang^[†]
School of Pharmacy
Hunan University of Chinese Medicine
Changsha 410208, China

Prof. G. B. Ge^[†]
Institute of Interdisciplinary Integrative Medicine Research
Shanghai University of Traditional Chinese Medicine
Shanghai, 201203, China

Prof. T. D. James
Department of Chemistry
University of Bath
Bath BA2 7AY, United Kingdom

[†] These authors contributed equally.
Supporting information for this article is given via a link at the end of the document.



Scheme 1. Two-dimensional strategy to develop a two-photon fluorescent probe for CYP3A4. **A.** In the first dimension, an in-house docking program was used to perform the constrained virtual screening of 58 putative two-photon fluorophores with the curated CYP3A4 receptor ensemble, and **NN** was identified as the most promising fluorescent substrate for CYP3A4. **B.** In the second dimensional design, the chemical modification at a nitrogen atom of **NN** was carried out to optimize the reaction rate and isoform-selectivity of **NN** activation by 4-hydroxylation. The CYP isoform-selectivity of 18 **NN** derivatives was shown as an insert. The brightness of green represents the rate of activation of **NN** derivatives by different subtypes of CYPs. The derivative **2 (NN 2, NEN)** displayed the great reactivity and high selectivity toward CYP3A4 over other CYPs isoforms.

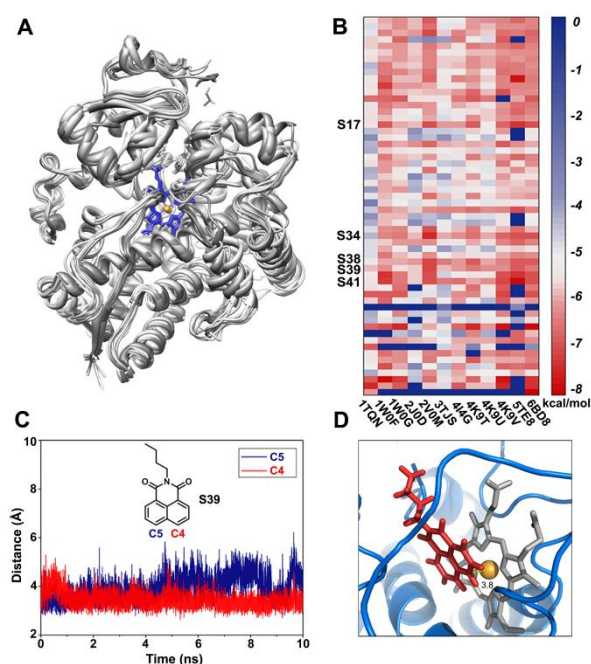


Figure 1. Computational screening and discovery of fluorescent substrates for CYP3A4. **(A)** Overlay of twelve structurally diverse CYP3A4 structures as the receptor ensemble for virtual screening. **(B)** The heatmap derived from the virtual screening against the receptor ensemble consisting of 12 binding scores for each of 58 substrates. **(C)** The distance of C4 atom (catalytic site) as well as C5 atom of **S39** with Fe of heme (C-Fe) along the time trajectory during 10 ns position constrained MD simulations. **(D)** **S39** displayed in red stick binding in the

catalytic site of CYP3A4 structure derived from constrained MD simulation.

414G, 4K9T, 4K9U, 4K9V, 5TE8 and 6BD8) as the receptor ensemble for virtual screening during which the given catalytic sites of these substrates were constrained to 4.5 Å from the Fe atom of the heme (C-Fe). For each lead fluorophore, the receptor ensemble will generate a binding spectrum with twelve binding scores. The mean value of the binding scores were recorded and used to rank these substrates of CYP3A4. We selected top 5 ranked CYP3A4 substrates which were then subjected to further constrained molecular dynamics simulation and free energy calculation using the Poisson–Boltzmann surface area continuum solvation (MM/PBSA) methods (Table S1). Lastly, N-n-butyl-1,8-naphthalimide with the hydroxylation of C-4, stands out as the optimal candidate with the best binding free energy in the screening campaign (Figure 1). N-butyl and N-phenyl derivatives of naphthalimide (**NN**) were synthesized to verify the virtual screening results. It found that CYP3A4 could hydroxylate the two derivatives and caused remarkable fluorescence enhancement at 558 nm (Figure S2, S3). This result suggested that the first step in molecular design for rapidly screening fluorophore structures was very efficient.

Finally, **NN** was selected as the fluorophore in the present study, because it possesses CYP3A4 preference and desirable photophysical properties, such as high photostability and significant two-photon absorbability at the near infrared wavelengths.^[15] Hydroxylation at C-4 triggers significant change in the fluorescence spectra, which makes **NN** a desirable OFF-ON two-photon fluorescent probe based on the mechanism of internal charge transfer (ICT).^[16] CYP1As and isoforms of other subfamily did not participate in the hydroxylation with the disappearance of emission at 558 nm. However, it can still be hydroxylated by CYP3A5, a highly homologous isoform of CYP3A4.^[17]

Subsequently, according to the structural features of **NN** and CYP3A4 catalytic cavity, we introduced various substituent groups to non-reaction site of **NN**, to adjust the reactive rate and isoform-selectivity (Figure S2), all of which construct our secondary design dimension. Briefly, the nitrogen atom of **NN** was selected as the modification site to introduce the substituents including steric bulk, hydrophilic and hydrophobic groups. A library of **NN** derivatives (**NN 1–18**) were synthesized to evaluate their potential as selective substrates for CYP3A4 by reaction phenotyping-based experimental screening (Figure S2). When introducing the benzene and its analogues to nitrogen atom of **NN** (**NN 10–13**), the reactive rates and isoform-selectivity were decreased. Introducing the hydrophobic substituents including alkanes with different lengths, some short-chain alkyl derivatives such as **NN 1** (methyl) and **NN 2** (ethyl) exhibited good reactivity and high specificity toward CYP3A4, rather than other derivatives with long-chain alkanes (**NN 3–9**). Additionally, the hydrophilic substituents (**NN 15–18**) also decreased the reaction rates. N-ethyl-1,8-naphthalimide (**NEN, NN 2**) displayed a good reactivity and high selectivity toward CYP3A4 over the other isoforms (Figure S3). Subsequently, we explore the feasibility and practicability of this activatable fluorescence method in the complex biological systems, and thereby examine our two-dimension molecular design strategy.

The specificity of **NEN** for CYP3A4 was firstly investigated. As shown in Figure 2B, CYP3A4 caused remarkable fluorescence enhancement at 558 nm, whereas there was no obvious

fluorescence changes upon addition of other CYP isoforms. Moreover, **NEN** exhibits high selectivity for CYP3A4 over various

protein content in HLM. The activity for **NEN** 4-hydroxylation was expressed by the formation rate of **NEHN**. $\lambda_{\text{ex}}/\lambda_{\text{em}} = 450/558 \text{ nm}$.

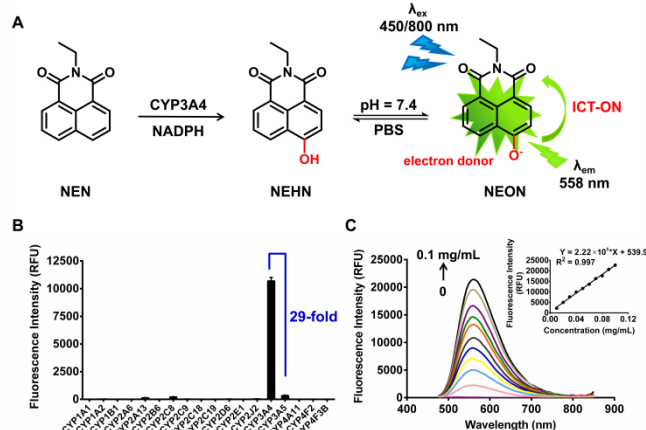


Figure 2. Fluorescence response of **NEN** towards CYP3A4. A) Proposed mechanism of CYP3A4 triggering the fluorescence response of **NEN**. B) Fluorescence response of **NEN** (10 μM) following incubation with various human CYPs. C) Fluorescence spectra of **NEN** (10 μM) following incubation with increasing concentrations of CYP3A4. CYP3A4 dependent fluorescence intensity change at 558 nm is shown as an inset.

potential interfering species (Figure S4). To further verify the selectivity of **NEN**, inhibition assays were conducted in human liver microsome (HLM) using some selective inhibitors of CYP isoforms. The hydroxylation of **NEN** can be strongly inhibited by CYP3cide and ketoconazole (TKZ), which are selective and potent inhibitors of CYP3A4 (Figure S5).^[18] These results indicated that **NEN** was highly selective for CYP3A4.

The metabolite of **NEN** was identified as N-ethyl-4-hydroxy-1,8-naphthalimide (**NEHN**, $\Phi_{\text{H}} = 0.199$ in PBS:ACN, $v/v = 1:1$) by CYP3A4, by comparison of LC retention times, UV and MS spectra with those of a standard compound (Figure S6). **NEN** showed extremely weak fluorescence over a wide pH range, while **NEHN** showed strong fluorescence with maxima at 558 nm over pH range of 7–12 (Figure S7). As a result, CYP3A4-mediated 4-hydroxylation of **NEN** led to discernible changes in the fluorescence emission (Figure 2A). The fluorescence intensity increased linearly when CYP3A4 was progressively added from 0 to 0.1 mg/mL ($R^2 = 0.997$, $Y = 2.22 \times 10^5 \cdot x + 539.9$) (Figure 2C). To understand the interaction between **NEN** and CYP3A4, the kinetics was assayed. As shown in Table S2 and Figure S8, **NEN** 4-hydroxylation in CYP3A4 and HLM followed the classic Michaelis–Menten kinetics, and displayed high affinity and good reactivity. However, the catalytic efficiency of CYP3A5 was very low, with at least 55-fold lower inherent clearance ($V_{\text{m}}/K_{\text{m}}$) than CYP3A4. The preferred characteristics and ideal kinetic behavior of probe reaction prompting

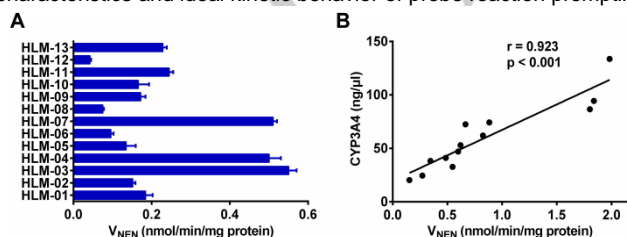


Figure 3. A) The catalytic activity of CYP3A4 in 13 individual HLM using **NEN** as the probe. B) Correlation between reactivity and the CYP3A4

us to use this probe for quantitative measurement of CYP3A4 activity.

Using **NEN**, the catalytic activity of CYP3A4 in a panel of 13 individual HLM can be efficiently determined (Figure 3A). More than 11-fold variation in the catalytic activity was observed. These data were compared with catalytic activity and protein content of CYP3A4 in the corresponding HLM, and a strong positive correlation was observed (Figure 3B, S9).^[6] Moreover, the CYP3A4 activity of different tissue homogenates was consistent with the corresponding protein levels of CYP3A4 (Figure S10). These findings demonstrated that **NEN** could serve as a novel molecular tool for *in vitro* detecting CYP3A4 in biospecimens.

The high specificity and two-photon absorption properties of **NEN** make it possible to directly detect CYP3A4 activity in intact cells and tissues. To explore the feature, human primary hepatocytes, which express various CYP isoenzymes, were used as model cells. Human primary hepatocytes were loaded with **NEN** (50 μM) at 37 $^{\circ}\text{C}$ for 1 h, and an obvious fluorescence enhancement in cells was observed (Figure 4). CYP3A4 inhibition and induction assays were also performed, where the cells were treated with TKZ (50 μM) or rifampin (10 μM , an inducer of CYP3A4).^[19] TKZ pretreated cells exhibited a largely suppressed fluorescence, while the cells pretreated with rifampin exhibited an enhanced fluorescence. The HPLC analysis for detecting cell lysates showed that the production of **NEHN** was well corresponding to the fluorescence intensity in the cells of different treated groups (Figure S12). Additionally, the TP imaging of a rat liver slice showed the practicability of **NEN** for imaging CYP3A4 in deep tissues (Figure S13). The images at the various depths showed the distribution of CYP3A4. All these results demonstrated that **NEN** displayed good cell permeability and deep tissue penetration capability which were suitable for direct detecting endogenous CYP3A4 activity of cell and tissue.

Understanding and predicting whether new drug candidates will induce drug-drug interactions is a critical hurdle in pharmaceutical development.^[20] Encouraged by the above findings, we investigate the utility of **NEN** for high-throughput screening of CYP3A4 modulators *in vitro* and *in vivo*. One known chemical inhibitor of CYP3A4 (TKZ) was used to evaluate its inhibitory effects toward CYP3A4 in HLM and recombinant CYP3A4. TKZ inhibited **NEN** 4-hydroxylation in a dose-dependent manner with similar inhibitory tendency as determined in the two enzyme sources (Figure S15). Additionally, a known CYP3A4 inducer (dexamethasone, DEX) was used to evaluate its effects on the expression and activity of CYP3A4 in rat primary hepatocytes.^[19] After co-incubation with DEX for 3 days, cells showed a dose-dependent increase of fluorescence, corresponding to the elevated formation rate of **NEHN** and CYP3A4 content in the cell lysates (Figure S16). Hence, **NEN** could be used to screen and characterize the CYP3A4 modulators. Unlike general CYP3A4-detecting assays such as the previous probe reaction or antibody-based enzyme-linked immunosorbent assay, **NEN** provides a simple and rapid approach to selectively and real-time detect CYP3A4 activity in cells or crude proteomes.^[20]

Zebrafish is a relatively new model system for drug metabolism and toxicity studies, offering whole organism screening coupled with the potential for high-throughput screening.^[21] In our study, zebrafish larvae display a clear and strong fluorescence region, which

precisely corresponding to liver area of zebrafish (Figure 5A, a-c). Meanwhile, the inhibitory effect of TKZ demonstrated that **NEN**

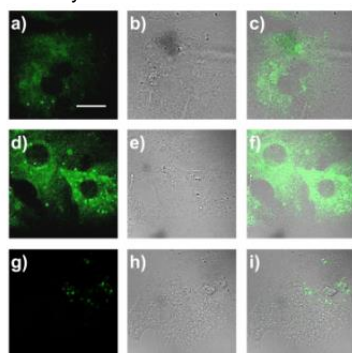


Figure 4. Two-photon confocal fluorescence images of CYP3A4 in human primary hepatocytes. Cells incubated with **NEN** (a-c); pretreated with rifampin (d-f); TKZ (g-i). (a, d, g) fluorescence images; (b, e, h) bright field images; (c, f, i) overlay images. Excitation: 800 nm, emission window: 520–560 nm.

measure the specific activity of CYP3A4 expressed in liver of zebrafish (Figure 5A, d-f). To examine whether **NEN** could faithfully report the drug-induced inhibition of CYP3A4 in living zebrafish, eight commonly used drugs (among which TKZ, indinavir and nilotinib are widely recognized CYP3A4 inhibitors, whereas others are not) are selected to co-incubate with **NEN** in zebrafish culture media.^[22] As shown in Figure 5B, the fluorescence intensity was evidently suppressed by three CYP3A4 inhibitors. Meanwhile, there was nearly no effect of known non-modulators of CYP3A4.^[23] When pretreated with 1 and 10 μ M indinavir, the fluorescence signal decreased to 37.1% and 16.8% of the control, implying the dose-dependent inhibitory effect of indinavir towards CYP3A4 (Figure

Excitation: 800 nm, emission window: 520–560 nm. Scale bar: 50 μ m. The pixel intensity from image (Ctrl) is defined as 1.0.

S17). Similarly, the phenomenon was observed in the TKZ- and nilotinib-treated group. Therefore, **NEN** displayed well tracking ability for CYP3A4 and faithfully reported the drug-induced inhibition of CYP3A4 in living zebrafish. **NEN** facilitates the rapid screening of CYP3A4 modulators and characterization of CYP3A4-mediated clinical drug interactions to assess risk of DDI caused by CYP3A4 inhibition.

In summary, using a two-dimensional molecular design strategy, we have successfully developed the first two-photon fluorescent probe for the selective detection of CYP3A4. **NEN** has been successfully applied for real-time imaging of CYP3A4 in various living systems, thereby providing a light-up readout to quantitatively characterize endogenous CYP3A4 activity *in vitro* and *in vivo*. Our practical strategy provides a novel approach for developing enzyme-activatable and isoform-specific fluorescent probes of target enzymes.

Acknowledgements

The authors thank the National Natural Science Foundation of China (81622047, 81503201, 81874301, 81473334 and 21572029), the Fundamental Research Funds for Central University (DLUT15QY43), the National Key R&D program of China (2018YFC1705900), the Distinguished Professor of Liaoning Province program, the Liaoning Revitalization Talents Program and State Key Laboratory of Fine Chemicals (KF1803) for financial support. T.D.J. wishes to thank the Royal Society for a Wolfson Research Merit Award.

Conflict of interest

The authors declare no conflict of interest.

Keywords: Analytical methods • Cytochrome P450 3A4 • Enzyme-activatable probe • Fluorescent probe • Molecular design strategy

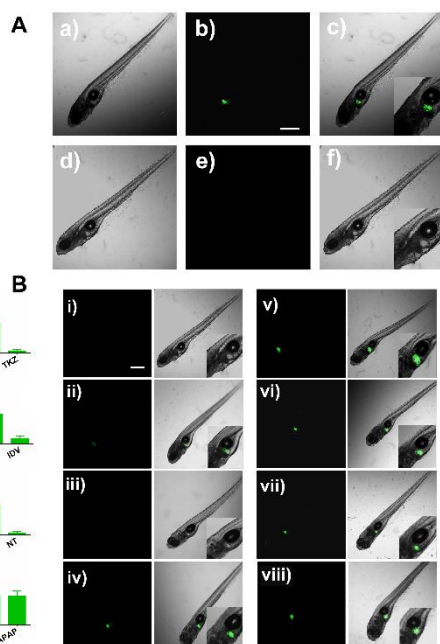


Figure 5. Fluorescence images of CYP3A4 in living zebrafish. Fish incubated with **NEN** (A-a, b, c); with **NEN** in the present of TKZ (A-d, e, f); with **NEN** in the present of clinical drugs (10 μ M) (B); i) TKZ; ii) indinavir, IDV; iii) nilotinib, NT; iv) acetaminophen, APAP; v) omeprazole, OME; vi) montelukast, MK; vii) sulfaphenazole, SZ; viii) clomethiazole, CZ. Magnified views are inserted in the corresponding overlay images.

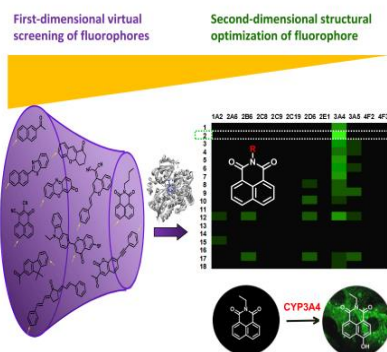
- [1] a) P. A. Williams, J. Cosme, D. M. Vinkovic, A. Ward, H. C. Angove, P. J. Day, C. Vonrhein, I. J. Tickle, H. Jhoti, *Science* **2004**, 305, 683–686; b) S. Rendic, F. J. Di Carlo, *Drug Metab. Rev.* **1997**, 29, 413–580; c) F. P. Guengerich, M. R. Waterman, M. Egli, *Trends Pharmacol. Sci.* **2016**, 37, 625–640.
- [2] a) T. Shimada, E. M. Gillam, P. Sandhu, Z. Guo, R. H. Tukey, F. P. Guengerich, *Carcinogenesis* **1994**, 15, 2523–2529; b) F. P. Guengerich, *Annu. Rev. Pharmacol. Toxicol.* **1999**, 39, 1–17.
- [3] a) R. Z. Harris, L. Z. Benet, J. B. Schwartz, *Drugs* **1995**, 50, 222–239; b) U. M. Zanger, M. Schwab, *Pharmacol. Ther.* **2013**, 138, 103–141.
- [4] a) P. H. Marathe, A. D. Rodrigues, *Methods Mol. Biol.* **2010**, 596, 385–403; b) P. Wei, J. Zhang, M. Egan-Hafley, S. Liang, D. D. Moore, *Nature* **2000**, 407, 920–923; c) H. N. Chaobal, E. D. Kharasch, *Clin. Pharmacol. Ther.* **2005**, 78, 529–539; d) B. Wassmur, J. Gräns, P. Kling, M. C. Aquat. *Toxicol.* **2010**, 100, 91–100.

- [5] T. Hirota, I. Ieiri, H. Takane, S. Maegawa, M. Hosokawa, K. Kobayashi, K. Chiba, E. Nanba, M. Oshimura, T. Sato, et al, *Hum. Mol. Genet.* **2004**, *13*, 2959-2969.
- [6] G. B. Ge, J. Ning, L. H. Hu, Z. R. Dai, J. Hou, Y. F. Cao, Z. W. Yu, C. Z. Ai, J. K. Gu, X. C. Ma, et al, *Chem. Commun.* **2013**, *49*, 9779-9781.
- [7] J. Wu, Y. Cao, Y. Zhang, Y. Liu, J. Y. Hong, L. Zhu, G. Ge, L. Yang, *Drug Metab. Dispos.* **2014**, *42*, 94-104.
- [8] a) J. Yan, S. Lee, A. Zhang, J. Yoon, *Chem. Soc. Rev.* **2018**, *47*, 6900-6916; b) Z. R. Dai, G. B. Ge, L. Feng, J. Ning, L. H. Hu, Q. Jin, D. D. Wang, X. Lv, T. Y. Dou, J. N. Cui, et al, *J. Am. Chem. Soc.* **2015**, *137*, 14488-14495; c) M. H. Lee, N. Park, C. Yi, J. H. Han, J. H. Hong, K. P. Kim, D. H. Kang, J. L. Sessler, C. Kang, J. S. Kim, *J. Am. Chem. Soc.* **2014**, *136*, 14136-14142; d) X. Wu, W. Shi, X. Li, H. Ma, *Angew Chem. Int. Ed. Engl.* **2017**, *56*, 15319-15323; e) X. He, L. Li, Y. Fang, W. Shi, X. Li, H. Ma, *Chem. Sci.* **2017**, *8*, 3479-3483; f) J. Ning, P. P. Dong, W. Wang, G. B. Ge, B. Wang, Z. L. Yu, L. Shi, X. G. Tian, X. K. Huo, L. Feng, et al, *J. Am. Chem. Soc.* **2019**, *141*, 1126-1134.; g) H. W. Liu, L. L. Chen, C. Y. Xu, Z. Li, H. Y. Zhang, X. B. Zhang, W. H. Tan, *Chem. Soc. Rev.* **2018**, *47*, 7140-7180.
- [9] a) L. Zhou, X. Zhang, Q. Wang, Y. Lv, G. Mao, A. Luo, Y. Wu, Y. Wu, J. Zhang, W. Tan, *J. Am. Chem. Soc.* **2014**, *136*, 9838-9841; b) Q. Xu, C. H. Heo, G. Kim, H. W. Lee, H. M. Kim, J. Yoon, *Angew. Chem. Int. Ed. Engl.* **2015**, *54*, 4890-4894.
- [10] a) A. B. Renwick, D. F. Lewis, S. Fulford, D. Surry, B. Williams, P. D. Worboys, X. Cai, R. W. Wang, R. J. Price, B. G. Lake, et al, *Xenobiotica* **2001**, *31*, 187-204; b) D. M. Stresser, S. D. Turner, A. P. Blanchard, V. P. Miller, C. L. Crespi, *Drug Metab. Dispos.* **2002**, *30*, 845-852.
- [11] S. Sansen, J. K. Yano, R. L. Reynald, G. A. Schoch, K. J. Griffin, C. D. Stout, E. F. Johnson, *J. Biol. Chem.* **2007**, *282*, 14348-14355.
- [12] H. Z. Bu, *Curr. Drug Metab.* **2006**, *7*, 231-249.
- [13] J. Chan, S. C. Dodani, C. J. Chang, *Nat. Chem.* **2012**, *4*, 973-984.
- [14] Y. Liu, L. Zhao, W. Li, D. Zhao, M. Song, Y. Yang, *J. Comput. Chem.* **2013**, *34*, 67-75.
- [15] a) G. Loving, B. Imperiali, *J. Am. Chem. Soc.* **2008**, *130*, 13630-13638; b) M. H. Lee, J. H. Han, J. H. Lee, H. G. Choi, C. Kang, J. S. Kim, *J. Am. Chem. Soc.* **2012**, *134*, 17314-17319; c) G. Liu, G. Shi, H. Sheng, Y. Jiang, H. Liang, S. Liu, *Angew. Chem. Int. Ed. Engl.* **2017**, *56*, 8686-8691.
- [16] D. Srikun, E. W. Miller, D. W. Domaille, C. J. Chang, *J. Am. Chem. Soc.* **2008**, *130*, 4596-4597.
- [17] a) P. Kuehl, J. Zhang, Y. Lin, J. Lamba, M. Assem, J. Schuetz, P. B. Watkins, A. Daly, S. A. Wrighton, S. D. Hall, et al, *Nat. Genet.* **2001**, *27*, 383-391; b) M. H. Hsu, U. Savas, E. F. Johnson, *Mol. Pharmacol.* **2018**, *93*, 14-24.
- [18] a) S. Dilmaghanian, J. G. Gerber, S. G. Filler, A. Sanchez, J. Gal, *Chirality* **2004**, *16*, 79-85; b) R. L. Walsky, R. S. Obach, R. Hyland, P. Kang, S. Zhou, M. West, K. F. Geoghegan, C. J. Helal, G. S. Walker, T. C. Goosen, et al, *Drug Metab. Dispos.* **2012**, *40*, 1686-1697.
- [19] T. A. Kocarek, E. G. Schuetz, S. C. Strom, R. A. Fisher, P. S. Guzelian, *Drug Metab. Dispos.* **1995**, *23*, 415-421.
- [20] a) C. D. Scripture, W. D. Figg, *Nat. Rev. Cancer* **2006**, *6*, 546-558; b) A. Kamel, S. Harriman, *Drug Discov. Today Technol.* **2013**, *10*, 177-189.
- [21] A. Hill, N. Mesens, M. Steemans, J. J. Xu, M. D. Aleo, *Drug Metab. Rev.* **2012**, *44*, 127-140.
- [22] a) V. A. Eagling, D. J. Back, M. G. Barry, *Br. J. Clin. Pharmacol.* **1997**, *44*, 190-194; b) A. M. Filppula, P. J. Neuvonen, J. T. Backman, *Drug Metab. Dispos.* **2014**, *42*, 1202-1209.
- [23] a) G. Langdon, J. Davis, G. Layton, C. L. Chong, G. Weissgerber, M. Vourvahis, *Br. J. Clin. Pharmacol.* **2012**, *73*, 768-775; b) H. Zhang, J. Sheng, J. H. Ko, C. Zheng, W. Zhou, P. Priess, W. Lin, S. Novick, *J. Clin. Pharmacol.* **2015**, *55*, 401-408.

COMMUNICATION

Selective two-photon CYP3A4

probe: A highly sensitive two-photon fluorescent probe specific for CYP3A4 was designed based on a two-dimension design strategy that combined ensemble-based virtual screening with rationally structure modification. Facilitating the detection of CYP3A4 activity in living cell, tissue and zebrafish, allowing for the evaluation of risks from CYP3A4-mediated drug-drug interactions in the clinic.



J. Ning, W. Wang, G. B. Ge, P. Chu, F. D. Long, Y. L. Yang,* Y. L. Peng, L. Feng,* X. C. Ma* and T. D. James

Page No. – Page No.

Targeted Enzyme Activated Two-Photon Fluorescent Probes: A Case Study of CYP3A4 Using a Two-Dimensional Design Strategy